Original Paper

phys. stat. sol. (b) **242**, No. 8, 1719–1727 (2005) / **DOI** 10.1002/pssb.200440052

Magnetic and transport properties of the Co-doped manganite $La_{0.7}Sr_{0.3}Mn_{1-x}Co_xO_3$ ($0 \le x \le 0.5$)

B. C. Zhao[1], **W. H. Song**[1], **Y. Q. Ma**[1], **R. L. Zhang**[1], **J. Yang**[1], **Z. G. Sheng**[1], **W. J. Lu**[1], **J. M. Dai**[1], and **Y. P. Sun**[*, 1, 2]

[1] Key Laboratory of Materials Physics, Institute of Solid State Physics, Chinese Academy of Sciences, Hefei 230031, China

[2] National Laboratory of Solid State Microstructures, Nanjing University, Nanjing 210008, China

Received 31 October 2004, revised 11 April 2005, accepted 26 April 2005
Published online 9 June 2005

PACS 71.30.+h, 75.30.Kz, 75.47.Lx

The effect of Co doping on the magnetic and transport properties of $La_{0.7}Sr_{0.3}Mn_{1-x}Co_xO_3$ ($0 \le x \le 0.5$) is investigated. The Co doping at Mn sites dilutes the double-exchange interaction between Mn^{3+} and Mn^{4+} ions and changes the long-range ferromagnetic (FM) order of $La_{0.7}Sr_{0.3}MnO_3$ (LSMO) to the spin glass (SG) or cluster glass (CG) state for samples with $x \ge 0.1$. For $x \ge 0.3$, the paramagnetic (PM) metal to FM metal transition of LSMO disappears and the temperature dependence of resistivity $\rho(T)$ follows semiconducting behavior in the whole measured temperature region with the resistivity increasing by orders of magnitude. An interesting result is that $\rho(T)$ exhibits an obvious anomaly at $T^* \sim 100$ K, which is ascribed to the spin-state transition of Co ions. For samples with $x = 0.1$ and 0.3, magnetoresistance (MR) effects are markedly enhanced in the low-temperature region compared with undoped LSMO, which is suggested to originate from the appearance of spin-dependent tunneling magnetoresistance. However, for samples with $x = 0.5$, the MR effect is suppressed over the entire temperature region measured and an obvious exchange anisotropy phenomenon, characterized by the shift of the hysteresis loop, is also observed, which is ascribed to the marked increase of the antiferromagnetic insulating phase.

1 Introduction

The mixed valence perovskite manganites $R_{1-x}A_xMnO_3$ (where R = La–Tb, and A = Ca, Sr, Ba, Pb, etc.) have attracted much renewed attention due to the discovery of colossal magnetoresistance (CMR) [1–4]. Many theories have been proposed to explain the mechanism of CMR, such as double exchange (DE) [5], polaronic effects [6] and phase separation combined with percolation [7]. These theories suggest that the mixed valence of Mn^{3+}/Mn^{4+} is a key component for understanding the CMR effect and the transition from the paramagnetic (PM) insulator–ferromagnetic (FM) metal.

To understand the CMR mechanism, it is very important to perform investigations into the doping of transition elements at Mn sites because of the core role of Mn ions in CMR materials. Mn site doping effects of transition elements have been extensively investigated [8, 9]. As is well known, Co ions in perovskite-structure cobaltites can exist in three kinds of spin states, i.e. low spin (LS), intermediate spin (IS) and high spin (HS), due to the fact that the crystal field splitting (10 Dq) of the Co d states (E_{cf}) and Hund's rule coupling energy (E_{ex}) are comparable for the cobaltites. The fact that E_{cf} and E_{ex} are comparable means that the thermal energy ($k_BT \sim 10$ meV) can induce the spin-state transition of Co ions by thermal excitation of the t_{2g} electrons into e_g states [10]. Therefore, among all transition elements doping

* Corresponding author: e-mail: ypsun@issp.ac.cn

at Mn sites in perovskite-structure manganites, Co doping is more interesting because of the three kinds of spin states of Co ions and the spin-state transition. However, there exist some open issues. Firstly, whether the spin-state transition still exists for Co-doped manganites. Secondly, if it does, what is the effect of the spin-state transition on the magnetic and electronic transport properties of manganites? In a study of $La_{0.7}Ca_{0.3}Mn_{1-x}Co_xO_3$, Gayathri et al. did not observe the effect of the spin-state transition of Co ions [11]. However, very recently, Srivastava et al. report that there is evidence of the spin-state transition of Co ions for compounds with similar compositions [12].

Therefore, to understand further the effect of Co-doping at Mn sites in manganites, in the present paper we report an investigation of the magnetic and transport properties of $La_{0.7}Sr_{0.3}Mn_{1-x}Co_xO_3$ ($0 \le x \le 0.5$) polycrystalline samples.

2 Experimental

$La_{0.7}Sr_{0.3}Mn_{1-x}Co_xO_3$ (x = 0, 0.01, 0.1, 0.3, 0.5) bulk samples were prepared by the conventional solid-state reaction method. Well-mixed stoichiometric amounts of high-purity La_2O_3, $SrCO_3$, MnO_2 and Co_2O_3 powders were calcined at 1000 and 1200 °C for 24 h each with an intermediate grinding. The powders obtained were ground, pelletized and sintered at 1350 °C for 24 h with three intermediate grindings. Finally, the furnace was cooled to room temperature.

The structure and phase purity of the samples were examined by powder X-ray diffraction (XRD) using a Philips X'pert PRO X-ray diffractometer with CuK_α radiation at room temperature. The magnetic measurements were performed using a Quantum Design superconducting quantum interference device (SQUID) MPMS system ($2 \le T \le 400$ K, $0 \le H \le 5$ T). The resistance was measured using the standard four-probe method from 5 to 390 K in an applied field in the range $0 \le H \le 5$ T.

3 Results and discussion

The XRD patterns at room temperature shown in Fig. 1 indicate that all samples of $La_{0.7}Sr_{0.3}Mn_{1-x}Co_xO_3$ (x = 0, 0.01, 0.1, 0.3, 0.5) are of the same structure. All peaks can be indexed with a rhombohedral structure with space group $R\bar{3}c$ (no. 167) over the whole doping concentration range. The relevant structural parameters obtained by fitting the experimental spectra using the Rietveld refinement technique [13] are listed in Table 1. The Co doping does not change the crystal structure, but the Mn–O bond length and

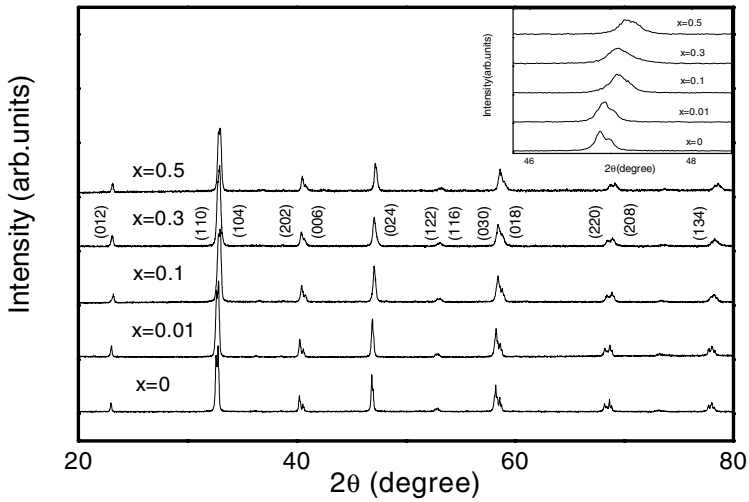

Fig. 1 X-ray diffraction patterns for $La_{0.7}Sr_{0.3}Mn_{1-x}Co_xO_3$ (x = 0, 0.01, 0.1, 0.3, 0.5) samples. The inset shows the shift of the (024) peaks due to variation of the Co doping concentration.

Table 1 Refined structural parameters of $La_{0.7}Sr_{0.3}Mn_{1-x}Co_xO_3$ ($0 \le x \le 0.5$) at room temperature. The space group is $R\bar{3}c$.

	$x = 0$	$x = 0.01$	$x = 0.1$	$x = 0.3$	$x = 0.5$
a (Å)	5.5037	5.5045	5.5001	5.4776	5.4688
c (Å)	13.3657	13.3678	13.350	13.3058	13.2820
V (Å^3)	350.609	350.69	349.746	345.742	344.017
Mn–O (Å)	1.960	1.961	1.958	1.951	1.947
∠Mn–O–Mn (°)	163.86	163.86	163.85	163.86	163.86
R_p (%)	8.869	7.965	7.881	6.152	5.661

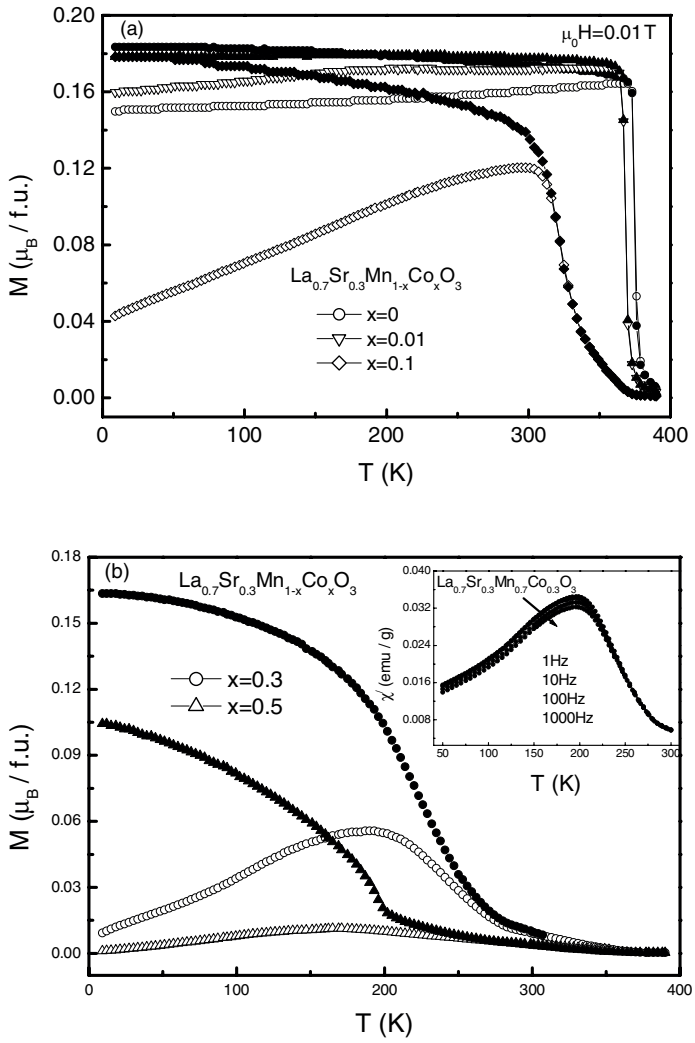

Fig. 2 Temperature dependence of dc magnetization measured at 0.01 T for $La_{0.7}Sr_{0.3}Mn_{1-x}Co_xO_3$: a) $x = 0$, 0.01 and 0.1; b) $x = 0.3$ and 0.5. The open symbols represent the ZFC data and the filled symbols the FC data. The arrow denotes the freezing temperature T_f (see text). The inset shows the ac susceptibility (χ') of $La_{0.7}Sr_{0.3}Mn_{0.7}Co_{0.3}O_3$.

the unit cell volume increase initially for the sample with $x = 0.01$ and then decrease with increasing Co doping content. The results are consistent with the fact that the Co ion has a smaller ionic radius. However, Co doping has little influence on the Mn–O–Mn bond angle.

The temperature dependence of the dc magnetization $M(T)$ measured in the zero-field-cooled (ZFC) and field-cooled (FC) modes at an applied field of 0.01 T is shown in Fig. 2 for all samples. The Curie temperature T_C (defined as the peak temperature of the dM/dT vs. T curve) as well as the low-temperature magnetization decrease monotonically with increasing Co doping level. It is noteworthy that T_C shows a rapid drop even with a very small amount of Co doping (from 376 K for undoped $La_{0.7}Sr_{0.3}MnO_3$ (LSMO) to 367 K for the doped sample with $x = 0.01$). However, the $M(T)$ curve of the $x = 0.01$ sample is rather similar to that of the undoped LSMO, i.e. they both show a sharp PM to FM transition. For $x \geq 0.1$, the PM–FM phase transition becomes broader with increasing Co doping level implying the appearance of magnetic inhomogeneity. This kind of magnetic inhomogeneity is also shown by an obvious deviation between the FC and ZFC magnetization curves below a certain temperature (defined here as the freezing temperature, T_f) for the samples with $x \geq 0.1$. The phenomenon of the discrepancy between FC and ZFC magnetization curves is usually ascribed to the appearance of the spin glass (SG) or cluster glass (CG) state induced by the competing interaction between FM and antiferromagnetic (AFM) exchange interaction. The glass state can be further proved by the temperature dependence of the ac susceptibility χ' as shown in the inset of Fig. 2b: the susceptibility becomes frequency dependent below T_f. Figure 2 shows that the deviation between FC and ZFC magnetization curves becomes larger and T_f shifts to lower temperature with increasing Co doping level, implying an enhanced AFM exchange interaction due to increased Co doping at Mn sites.

In order to analyze quantitatively the variation of the magnetic susceptibility due to Co doping, we plot the temperature dependence of the inverse of χ, i.e. $\chi^{-1}(T)$, and observe that $\chi^{-1}(T)$ follows the Curie–Weiss law well above T_C for all samples except for $x = 0.5$. By fitting $\chi^{-1}(T)$ according to the Curie–Weiss law, $\chi^{-1}(T) = 3k_B(T - \Theta)N_0^{-1}\mu_{eff}^{-2}$, where k_B, N_0, μ_{eff} and Θ are the Boltzmann constant, Avogadro's constant, the effective magnetic moment and the Weiss temperature, respectively, μ_{eff} and Θ are obtained [14]. The variation of μ_{eff} and Θ with Co doping level x is listed in Table 2. This shows that both μ_{eff} and Θ decrease with increasing Co doping level, which means a weakening of the FM DE interaction between Mn^{3+} and Mn^{4+} caused by Co doping.

The field dependence of the magnetization at 5 K is shown in Fig. 3. It can be seen that for the samples with $x = 0$ and 0.01, the magnetization reaches saturation at about 1 T and remains almost constant up to 5 T, which is considered a result of the rotation of the magnetic domain under the action of the applied magnetic field. The value of the saturated magnetic moment for the sample with $x = 0$ and 0.01 (4.06 and $3.84\mu_B$/f.u.) is higher than the expected one ($3.7\mu_B$/f.u.) for the spin-only contribution with

Table 2 Magnetic and electric parameters for $La_{0.7}Sr_{0.3}Mn_{1-x}Co_xO_3$ ($0 \leq x \leq 0.5$).

parameter	$x = 0$	$x = 0.01$	$x = 0.1$	$x = 0.3$	$x = 0.5$
T_C (K)	376	367	322	210	195
μ_{eff} (μ_B)	5.70	5.48	3.45	2.67	–
Θ (K)	373	369	361	353	–
M_{5T} (μ_B)	4.06	3.84	3.27	2.96	0.74
M_{re}/M_{5T}	–	0.004	0.09	0.29	0.31
H_c (T)	–	0.0009	0.024	0.081	0.322
T_p (K)	374	369	–	–	–
$T_0^h(0)$	–	–	1.48×10^5	4.90×10^6	7.24×10^7
$T_0^h(H)$	–	–	–	2.28×10^6	6.65×10^7
$T_0^l(0)$	–	–	–	9.17	–
$T_0^h(H)$	–	–	–	8.83	–

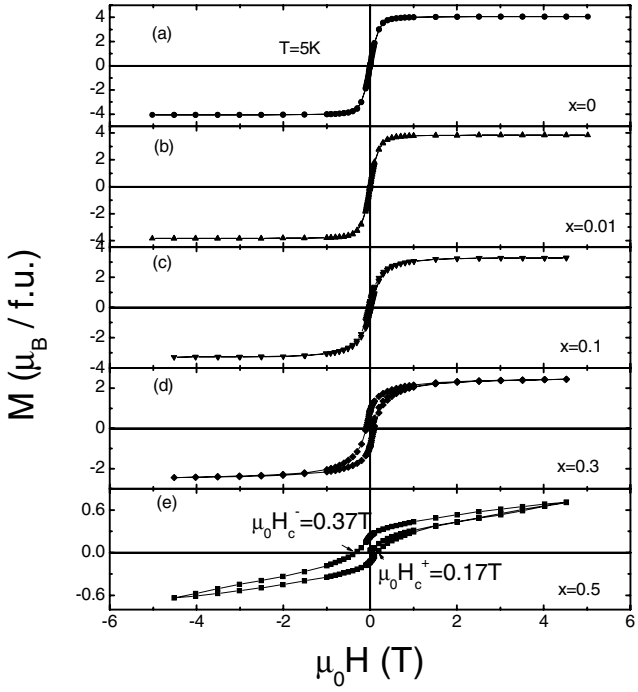

Fig. 3 Field dependence of dc magnetization for $La_{0.7}Sr_{0.3}Mn_{1-x}Co_xO_3$ at 5 K.

$g = 2$; a similar result has also been reported previously for this system [15, 16]. For the samples with $x = 0.1$, 0.3 and 0.5, the magnetization M increases linearly without saturation at higher fields implying the existence of the AFM phase. It is well known that the competition between FM and AFM phase would lead to the appearance of SG or CG states. This is why SG or CG behavior occurs in the samples with $x = 0.1$, 0.3 and 0.5. In addition, it is found that both the residual magnetization M_{re} and coercive force H_c are very small implying that the samples are good soft ferromagnets for $x = 0$ and 0.01, which behave with the same character as most manganites with optimal doping [17]. However, for $x \geq 0.1$, Fig. 3 indicates that the values of M_{re}/M_{5T} and H_c increase with Co doping level as shown in Table 2, where M_{5T} is the magnetization at an applied field of 5 T and at 5 K. The increase of M_{re}/M_{5T} and H_c is ascribed to originate from the increased AFM phase component and the pinning action of the AFM phase on the FM domains. The enhanced pinning action of the AFM phase can be further shown by the exchange anisotropy behavior as shown in Fig. 3 (curve e). This shows that the $M(H)$ hysteresis loop has a clear shift with $\mu_0 H_c^+ = 0.17$ T and $\mu_0 H_c^- = 0.37$ T at 5 K for the sample with $x = 0.5$.

As we know, Co enters manganite at low doping preferably as Co^{2+} and induces extra Mn^{4+} valence. Co ions in the perovskite structure exist in mixed valences of Co^{2+} and Co^{3+} similar to Mn ions [18]. Hence, as an example, the chemical formula for the sample with $x = 0.3$ can be written as $La_{0.7}Sr_{0.3}Mn^{3+}_{0.3}Mn^{4+}_{0.4}Co^{3+}_{0.2}Co^{2+}_{0.1}O_3$. That is to say, Co doping at Mn sites may introduce very complicated exchange interactions between Mn ions, Co ions, Mn and Co ions, etc., if we consider the three kinds of spin states of Co ions, i.e. LS, IS and HS. However, based on the above results of magnetization measurements, we find that the net effect of Co doping at Mn sites is to enhance the AFM exchange interaction and to weaken the DE interaction between Mn^{3+} and Mn^{4+}. In addition, the obvious effect of a possible spin-state transition of Co ions on the magnetization observed in perovskite-structure $LaCoO_3$ occurring near 100 K has not been found here for $La_{0.7}Sr_{0.3}Mn_{1-x}Co_xO_3$ for $M(T)$ curves.

To investigate the effect of Co doping at Mn sites on the electronic transport property of the samples, the temperature dependence of resistivity $\rho(T)$ was measured at zero applied field in the temperature

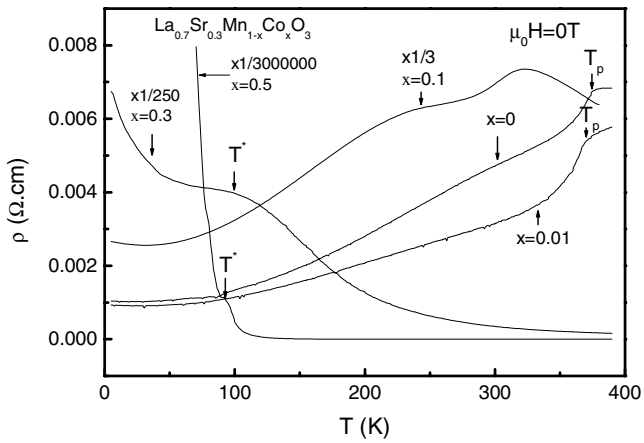

Fig. 4 Temperature dependence of the resistivity at zero field for $La_{0.7}Sr_{0.3}Mn_{1-x}Co_xO_3$ (x = 0, 0.01, 0.1, 0.3, 0.5). The resistivity is multiplied by 1/3, 1/250 and 1/300 000 for the samples with x = 0.1, 0.3 and 0.5, respectively.

range 5–390 K. The results are shown in Fig. 4. For the undoped LSMO sample, the slope of the $\rho(T)$ curve exhibits an obvious change at T_p = 374 K, which is close to the Curie temperature T_C (= 376 K) of the sample, in agreement with the previously reported result for LSMO [14]. That is to say, for LSMO, the transport mechanism occurs via a transition from PM metal to FM metal accompanying the PM–FM transition because of the larger bandwidth of e_g electrons and less electron–phonon interaction due to less lattice distortion. For the sample with x = 0.01, the ρ value is decreased compared with the LSMO sample and the T_C and T_p values are decreased due to the slight dilution of DE interaction between Mn^{3+} and Mn^{4+}. The decrease of ρ may be ascribed to the reduction of Jahn–Teller distortion of $Mn^{3+}O_6$ octahedra [19] and the change of the ratio of Mn^{3+} and Mn^{4+} due to the doping of Co^{2+} ions. For x = 0.1, Fig. 4 shows that there is an insulator–metal transition at about 321 K (near T_C). For the samples with $x \geq 0.3$, Fig. 4 shows that $\rho(T)$ shows semiconducting behavior throughout the measured temperature region with the resistivity increased by orders of magnitude. For $x \geq 0.3$, the Mn^{4+} preponderance due to Co doping is likely to be responsible for the change of manganite from FM metal to a phase-separate FM/AFM insulator where the transport occurs in the more conducting Co subsystem. In addition, the slope of the $\rho(T)$ curve behaves anomalously in the vicinity of 100 K (denoted T^* in Fig. 4). This anomaly can be observed more clearly by plotting the curve of ln (ρ) vs. $T^{-1/4}$ as shown in Fig. 5. As is well known, the Co

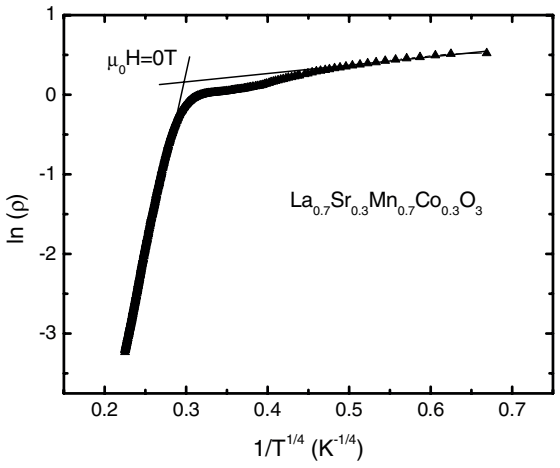

Fig. 5 Temperature dependence of the zero field resistivity plotted as ln (ρ) vs. $1/T^{1/4}$ for the sample with x = 0.3. The solid lines are fitting lines.

ion in perovskite-structure $LaCoO_3$ has a spin-state transition near 100 K [10]. It is suggested that the anomaly in the $\rho(T)$ curve may be related to the spin-state transition of Co ions.

To understand the transport mechanism of the studied samples clearly, $\rho(T)$ curves are fitted by the thermally activated (TA) law, $\rho \propto \exp(E_0/k_B T)$, the adiabatic small polaron hopping (SPH) model, $\rho \propto T \exp(E_p/k_B T)$, and the Mott variable range hopping (VRH) model, $\rho \sim \exp(T_0/T)^{1/4}$ [3]. The results indicate that $\rho(T)$ curves can be well described by the Mott VRH model in the high-temperature region for the $x = 0.1$, 0.3 and 0.5 samples and the low-temperature region ($T < 50$ K) for the sample with $x = 0.3$. That is to say, for Co-doped samples with $x \geq 0.3$, the disorder effect due to Co doping at Mn sites may dominate the transport property of carriers. By fitting, the fitting parameter $T_0(0)$ can be obtained, which has different values for high- and low-temperature regions, denoted $T_0^h(0)$ and $T_0^l(0)$. Both values for different samples are listed in Table 2. According to the Mott VRH formula expression, the value of $T_0(0)$ is given by $k_B T_0 = \alpha/[\xi^3 N(E_F)]$, where $N(E_F)$ is the density of electronic states at the Fermi energy level, ξ is the electron localization length and α is a numerical constant whose value is not precisely known but is usually taken as being in the range 18–21 [20, 21]. Table 2 shows that $T_0^h(0)$ increases markedly with Co doping level, implying a decrease of the localization length ξ provided $N(E_F)$ does not change. That is to say, the localization degree of the carriers increases with increasing Co doping level. In addition, for a fixed Co doping level, Table 2 shows that $T_0^h(0) >> T_0^l(0)$, meaning that the localization degree becomes significantly greater in the high-temperature region above T^* compared with that in the low-temperature region below T^*. We suggest that the variation of the localization degree near T^* originates from the spin-state transition of Co ions. That is to say, below T^*, Co ions lie in the LS state, i.e. for Co^{3+}, $S = 0$. Hence, the localization of carriers induced by spin disorder of Co ions does not occur. However, for $T > T^*$, the spin state of Co ions will show the transition from LS state to IS or HS state induced by temperature, which will introduce additional localization of carriers due to the spin disorder of Co ions. Therefore, we attribute the anomaly of the $\rho(T)$ curves in the vicinity of T^* to the spin-state transition of Co ions induced by the temperature. Although there is no obvious anomaly corresponding to

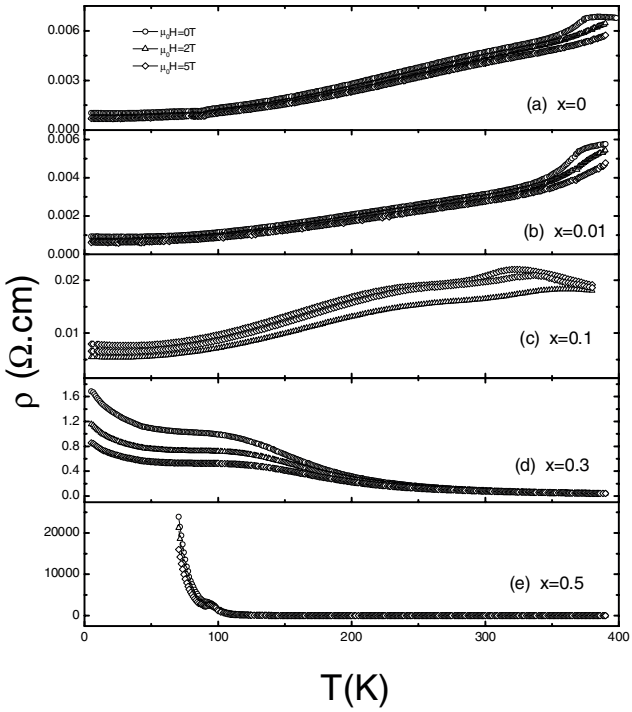

Fig. 6 Temperature dependence of resistivity under applied fields of $\mu_0 H = 0$, 2, 5 T for $La_{0.7}Sr_{0.3}Mn_{1-x}Co_xO_3$.

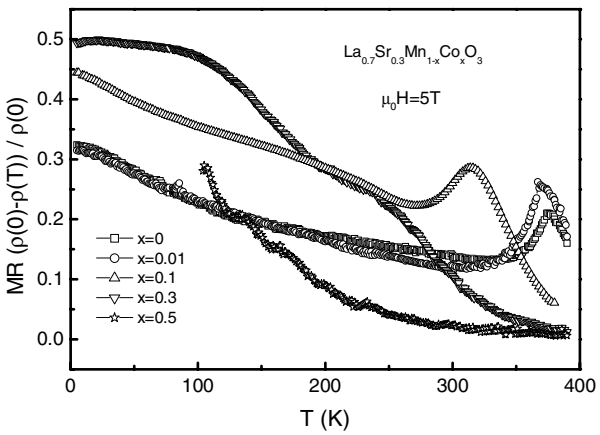

Fig. 7 Temperature dependence of magnetoresistance (MR) for $La_{0.7}Sr_{0.3}Mn_{1-x}Co_xO_3$ at $\mu_0 H = 5$ T.

T^* in the $M(T)$ curve which may be attributed to the strong exchange interaction between Mn ions, the change induced by the spin-state transition of Co ions may be spread out by the strong exchange interaction background between Mn ions. For the $x = 0.5$ sample, although the $\rho(T)$ curve in the high-temperature region above T^* can also be fitted in terms of the Mott VRH model, the $\rho(T)$ curve in the low-temperature region below T^* cannot be fitted by any existing model. This indicates that the transport mechanism of the $x = 0.5$ sample is different from that of the $x = 0.3$ sample, which is mainly ascribed to its markedly enhanced AFM interaction due to higher Co doping level.

The temperature dependence of resistivity $\rho(T)$ was also measured under the action of applied magnetic fields of 2 and 5 T for all samples as shown in Fig. 6. For all samples, $\rho(T)$ is markedly decreased under the action of a magnetic field and shows a magnetoresistance (MR) effect. We also fitted the $\rho(T)$ curves under the applied field of 5 T using the Mott VRH model for the samples with $x = 0.3$ and 0.5. The fitting parameters $T_0^h(H)$ and $T_0^l(H)$ are also listed in Table 2. The values of $T_0(H)$ decrease dramatically under the action of the applied field, meaning that the localization degree becomes less.

MR as a function of temperature is plotted in Fig. 7. Here MR is defined as MR = $[\rho(0) - \rho(5\text{T})]/\rho(0)$, where $\rho(0)$ is the resistivity at zero field and $\rho(5\text{T})$ is the resistivity at an applied magnetic field of 5 T. Figure 7 shows that MR of the samples with $x = 0$ and 0.01 exhibits an obvious peak around T_p originating from the suppression of intrinsic spin-dependent scattering within grains and increases with decreasing temperature below T_p stemming from spin-dependent scattering of grain boundaries [22]. For the sample with $x = 0.3$, Fig. 6 shows that $\rho(T)$ is markedly decreased under the action of magnetic fields and the temperature T^* at which ρ behaves anomalously under zero field shifts to high temperatures with increasing magnetic fields. That is to say, the temperature of the spin-state transition of Co ions increases with increasing magnetic field. The detailed reason of this kind of variation is not clear at present. In addition, Fig. 7 shows that there is no MR peak around T_C for the samples with $x \geq 0.3$, instead MR effects are markedy enhanced in the low-temperature region below T_C compared with undoped LSMO, which is ascribed to originate from the appearance of spin-dependent tunneling magnetoresistance (TMR). However, for the $x = 0.5$ sample, the MR effect is suppressed over almost the entire measured temperature region, which is ascribed to its markedly enhanced AFM interaction due to higher Co doping level.

4 Conclusions

We have presented detailed transport and magnetization measurements on $La_{0.7}Sr_{0.3}Mn_{1-x}Co_xO_3$ ($x = 0$, 0.01, 0.1, 0.3, 0.5) polycrystalline samples. The anomaly appearing in $\rho(T)$ in the vicinity of T^* may mean that there is a spin-state transition of Co ions for samples with $x \geq 0.3$. The DE interaction between Mn^{3+} and Mn^{4+} ions can be easily diluted by Co doping at Mn sites. For $x \geq 0.1$, the SG or CG state be-

gins to appear and PM metal to FM metal transition of LSMO disappears and $\rho(T)$ shows semiconducting behavior throughout the measured temperature region. For the samples with $x = 0.1$ and 0.3, MR effects are markedly enhanced in the low-temperature region below T_c compared with undoped LSMO, which is ascribed to originate from the occurrence of TMR. However, for the sample with $x = 0.5$, the MR effect is suppressed over the entire measured temperature range and an obvious exchange anisotropy phenomenon, characterized by the shift of the hysteresis loop, is also observed, which is ascribed to the marked increase of AFM insulating phase.

Acknowledgments This work was supported by the National Key Research under Contract No. 001CB610604, and the National Nature Science Foundation of China under Contract No. 10174085, 10374033, AnHui Province NSF Grant No. 03046201 and the Fundamental Bureau of the Chinese Academy of Sciences.

References

[1] R. von Helmolt, J. Wecker, B. Holzapfel, L. Schultz, and K. Samwer, Phys. Rev. Lett. **71**, 2331 (1993).
[2] A. P. Ramirez, J. Phys.: Condens. Matter **9**, 8171 (1997).
[3] J. M. D. Coey, M. Viret, and S. von Molnar, Adv. Phys. **48**, 167 (1999).
[4] M. B. Salamon and M. Jaime, Rev. Mod. Phys. **73**, 583 (2001).
[5] C. Zener, Phys. Rev. **82**, 403 (1951).
[6] A. J. Millis, P. B. Littlewood, and B. I. Shraiman, Phys. Rev. Lett. **74**, 5144 (1995).
[7] S. Mori, C. H. Chen, and S. W. Cheong, Phys. Rev. Lett. **81**, 3972 (1998).
M. Uehara et al., Nature **399**, 560 (1999).
[8] K. Ghosh, S. B. Ogale, R. Ramesh, R. L. Greene, and T. Venkatesan, Phys. Rev. B **59**, 533 (1999).
[9] M. M. Xavier, Jr., F. A. O. Cabral, J. H. de Araújo, C. Chesman, and T. Dumelow, Phys. Rev. B **63**, 012408 (2000).
[10] S. R. English, J. Wu, and C. Leighton, Phys. Rev. B **65**, 220407 (2002).
[11] N. Gayathri, A. K. Raychaudhuri, S. K. Tiwary, R. Gundakaram, A. Arulraj, and C. N. R. Rao, Phys. Rev. B **56**, 1345 (1997).
[12] C. M. Srivastava, S. Banerjee, T. K. GunduRao, A. K. Nigam, and D. Bahadur, J. Phys.: Condens. Matter **15**, 2375 (2003).
[13] D. B. Wiles and R. A. Young, J. Appl. Crystallogr. **14**, 149 (1981).
[14] E. M. Levin, S.-S. Hou, S. L. Bud'ko, and K. Schmidt-Rohr, J. Appl. Phys. **96**, 5085 (2004).
[15] H. Y. Hwang, S. W. Cheong, N. P. Ong, and B. Batlogg, Phys. Rev. Lett. **77**, 2041 (1996).
[16] J. Blasco, J. Garcia, and J. Stankiewicz, Phys. Rev. B **68**, 054421 (2003).
[17] R. W. Li, J. R. Sun, Q. A. Li, T. Zhu, S. Y. Zhang, and B. G. Shen, J. Appl. Phys. **93**, 8092 (2003).
[18] D. D. Khalyavin, M. Pekala, G. L. Bychkov, S. V. Shiryaev, S. N. Barilo, I. O. Troyanchuk, J. Mucha, H. Misiorek, R. Szymczak, M. Baran, and H. Szymczak, J. Phys.: Condens. Matter **15**, 925 (2003).
[19] G. H. Jonker, J. Appl. Phys. **37**, 1424 (1966).
[20] N. F. Mott, in: Metal–Insulator Transitions, 2nd edition (Taylor and Francis, New York, 1997).
[21] W. N. Shafarman, D. W. Koon, and T. G. Castner, Phys. Rev. B **40**, 1216 (1989).
[22] H. Yi and J. Yu, Phys. Rev. B **58**, 11123 (1998).